Bond Order Analysis Based on Laplacian of Electron Density in Fuzzy Overlap Space.

ARTICLE *in* THE JOURNAL OF PHYSICAL CHEMISTRY A · MARCH 2013

Impact Factor: 2.69 · DOI: 10.1021/jp4010345 · Source: PubMed

2 AUTHORS:

Tian Lu
Beijing Kein Research Center for Natural Scien…
31 PUBLICATIONS **873** CITATIONS
SEE PROFILE

Feiwu Chen
University of Science and Technology Beijing
27 PUBLICATIONS **921** CITATIONS
SEE PROFILE

THE JOURNAL OF PHYSICAL CHEMISTRY A

Article

pubs.acs.org/JPCA

Bond Order Analysis Based on the Laplacian of Electron Density in Fuzzy Overlap Space

Tian Lu and Feiwu Chen*

Department of Chemistry and Chemical Engineering, School of Chemistry and Biological Engineering, University of Science and Technology Beijing, Beijing 100083, People's Republic of China and Beijing Key Laboratory for Science and Application of Functional Molecular and Crystalline Materials, Beijing 100083, People's Republic of China

Supporting Information

ABSTRACT: Bond order is an important concept for understanding the nature of a chemical bond. In this work, we propose a novel definition of bond order, called the Laplacian bond order (LBO), which is defined as a scaled integral of negative parts of the Laplacian of electron density in fuzzy overlap space. Many remarkable features of LBO are exemplified by numerous structurally diverse molecules. It is shown that LBO has a direct correlation with the bond polarity, the bond dissociation energy, and the bond vibrational frequency. The dissociation behavior of LBO of the N−N bond in N_2 has been studied. Effects of the basis sets, theoretic methods, and geometrical conformations on LBO have also been investigated. Through comparisons, we discussed in details similarities and discrepancies among LBO, Mayer bond order, natural localized molecular orbital bond order, fuzzy overlap population, and electron density at bond critical points.

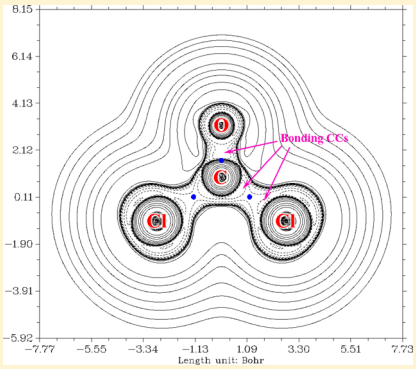

1. INTRODUCTION

The chemical bond is one of the key concepts in chemistry. Bond order is a quantitative description of chemical bonds and has been widely used by chemists to understand the nature of molecular electronic structure and predict the molecular reactivity, aromaticity, and stability. However, the chemical bond is unobservable, and there is also no unique way to define the bond order theoretically. There are a large number of definitions of bond order presented in the literature. Most of them are based on quantum mechanical properties such as Coulson bond order,[1] Wiberg bond order,[2] Mayer bond order (MBO),[3] Politzer bond order,[4−6] atomic overlap matrix bond order,[7] natural resonance theory bond order,[8] Nalewajski−Mrozek bond order,[9] effective bond order,[10] natural localized molecular orbitals bond order (NLMOBO),[11] delocalization index,[12−14] and fuzzy bond order.[15] Some others are based on experimental quantities such as equilibrium bond lengths and vibrational frequencies.[16] Very recently, it was argued that the bond order could be studied by noncontact atomic force microscopy.[17]

In ref 15, Mayer and Salvador not only proposed fuzzy bond order but also introduced the overlap population concept for "fuzzy atoms", which will be referred as the fuzzy overlap population (FOP) below. FOP can be written as[15]

$$\mathrm{FOP}_{A,B} = \int w_A(\mathbf{r}) w_B(\mathbf{r}) \rho(\mathbf{r})\, \mathrm{d}\mathbf{r} \tag{1}$$

where $\rho(\mathbf{r})$ denotes electron density at the point $\mathbf{r}$ and $w_A(\mathbf{r})$ stands for an atomic weighting function and corresponds directly to the scope of the atomic space. In principle, the atomic weighing function can be defined in an arbitrary way, as long as the following conditions can be satisfied

$$0 \le w_A(\mathbf{r}) \le 1 \quad \forall A, \forall \mathbf{r}$$
$$\sum_B w_B(\mathbf{r}) = 1 \quad \forall B, \forall \mathbf{r} \tag{2}$$

Atomic weighting functions can be classified into two categories:

(I) Fuzzy partitions. The common characteristic of this type of partition is that the atomic weighting function $w_A(\mathbf{r})$ goes from 1 to 0 smoothly as the variable $\mathbf{r}$ moves from one atom to other adjacent atoms. Hence, there are no clear boundaries between these atoms. Two of the most popular definitions in this category are proposed by Hirshfeld[18] and Becke.[19] The fuzzy partition scheme has been applied to bond order calculations,[15] population analysis[20,21] and orbital composition analysis.[22]

(II) Discrete partitions. The atomic weighting function of this partition is either 1 or 0 for adjacent atoms. The corresponding atomic spaces are therefore mutually exclusive with each other. Two typical representatives are the atoms in molecules (AIM) partition[23] and the Voronoi partition.[24] Because there are no overlap spaces between atoms under these partitions, FOP cannot be computed.

According to classical interpretations, formation of a covalent chemical bond originates from sharing electron pairs, which

Received: January 29, 2013
Revised: March 20, 2013
Published: March 20, 2013

   dx.doi.org/10.1021/jp4010345 | J. Phys. Chem. A 2013, 117, 3100−3108

results in a concentration of electron density between corresponding atoms. It naturally inspires one to think about the possibility to correlate FOP with bond order. This issue has already been explored by Oláh and co-workers.[25] They defined scaled FOP (sFOP) as follows

$$\mathrm{sFOP} = a \times \mathrm{FOP} + b \tag{3}$$

where a and b are parameters fitted against formal bond orders of C−C bonds in ethane, benzene, ethene, and ethyne. If Becke's partition is employed, a and b are equal to 10.55 and −1.90, respectively. sFOP does work well as a measure of bond order for a few organic molecules; however, sFOP cannot simply be regarded as a universal definition of bond order. For example, sFOP for the H−H bond in H_2 is −0.58. This result severely contradicts one's chemical intuition. If one wants to use sFOP to measure bond order for a wide variety of chemical bonds, multiple sets of parameters may have to be prefitted, and a suitable set should be properly chosen according to the various kinds of chemical bonds. Unfortunately, this is not a trivial task.

The Laplacian of electron density is defined as follows[23,26]

$$\nabla^2\rho(\mathbf{r}) = \frac{\partial^2\rho(\mathbf{r})}{\partial x^2} + \frac{\partial^2\rho(\mathbf{r})}{\partial y^2} + \frac{\partial^2\rho(\mathbf{r})}{\partial z^2} \tag{4}$$

Because minor variations of a function can be magnified by the Laplacian operator, this operator is capable of extracting much information of chemical interest from the electron density distribution. For example, $\nabla^2\rho$ has been used to reveal the atomic shell structure[27] and probe the S_N2 reaction path.[28] The positive and negative values of $\nabla^2\rho$ correspond to the electron density that is locally depleted and concentrated, respectively. It is well-known that if a covalent interaction occurs between two atoms, their valence electrons must be concentrated toward each other. This phenomena is known as bonding charge concentrations (bonding CCs).[26] As an example, the contour map of $\nabla^2\rho$ of $COCl_2$ is shown in Figure 1. Because of bonding CCs, the negative area of $\nabla^2\rho$ almost always presents in the atomic overlap region. Thus, it is reasonable to expect that the larger magnitude of the integral of negative $\nabla^2\rho$ in this region, the more intensive the bonding CC and, therefore, the stronger the covalent bonding. This is the theoretical basis of our new bond order based on $\nabla^2\rho$.

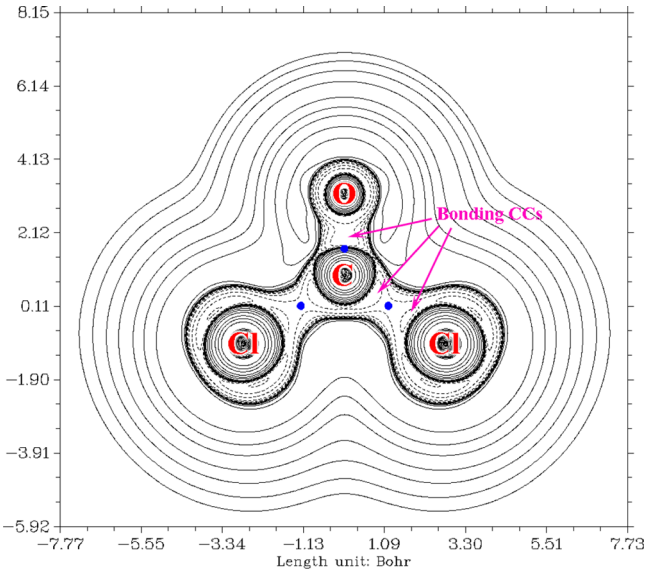

Figure 1. Contour map of $\nabla^2\rho$ of $COCl_2$. Solid and dashed lines correspond to positive and negative regions of $\nabla^2\rho$, respectively. Blue points correspond to bond critical points (BCPs). Some bonding charge concentration regions are highlighted by arrows.

In section 2, we introduce our new bond order. Section 3 includes computational and technical details. In section 4, we test our new bond order and compare it with other well-known bond order definitions. In the final section, we conclude this paper.

2. THEORY

The new bond order proposed here is named the Laplacian bond order (LBO) and is defined as

$$\mathrm{LBO}_{A,B} = -10 \times \int_{\nabla^2\rho<0} w_A(\mathbf{r}) w_B(\mathbf{r}) \nabla^2\rho(\mathbf{r})\, \mathrm{d}\mathbf{r} \tag{5}$$

Essentially, LBO is the integral of the negative part of $\nabla^2\rho$ in fuzzy overlap space. A simple prefactor −10 is introduced to make the magnitude of LBO consistent with one's chemical intuition for typical covalent bonds. This prefactor is determined empirically rather than being precisely fitted to some well-known bond orders.

In our current implementation, Becke's atomic weighting function with sharpness parameter $k = 3$ is employed; see the Supporting Information for a full description. The main advantages of Becke's definition are as follows: (1) The atomic spaces can easily be constructed. Neither spherical free-state atomic densities such as Hirshfeld partition nor iterations as in ISA partition[29] are required. (2) The distribution of the fuzzy overlap space can reasonably cover the whole bonding region if atomic radii are properly chosen, as discussed below.

Taking a diatomic molecule as an example, the Becke's atomic spaces and the corresponding overlap space are illustrated in Figure 2. Two red points denote the nuclear positions. Becke's weighting function implies the condition $d_A/d_B = R_A^{\mathrm{cov}}/R_B^{\mathrm{cov}}$, where R_A^{cov} and R_B^{cov} denote the covalent radius of the atoms A and B, respectively; d_A (d_B) is the distance between the nucleus A (B) and the position where the value of its corresponding weighting function w_A (w_B) is 0.5, as demonstrated in Figure 2. Apparently, the relative covalent radii directly affect the coverage of the overlap space. We found that for the existing covalent radii definitions,[30−33] the sizes of

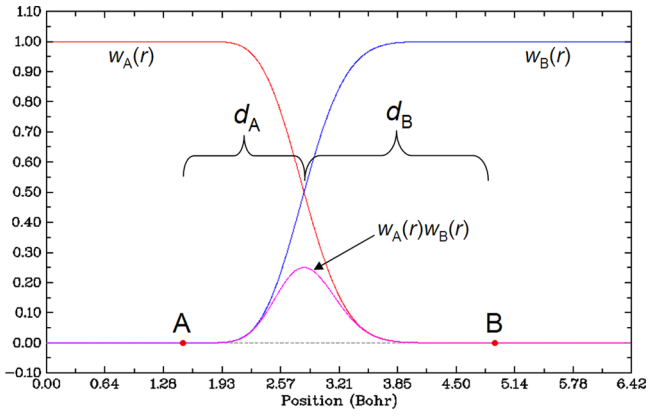

Figure 2. Illustration of Becke's atomic space and overlap space for a diatomic molecule; the sharpness parameter k is set to 3. Red points denote nuclear positions.

dx.doi.org/10.1021/jp4010345 | J. Phys. Chem. A 2013, 117, 3100−3108

Table 1. LBOs, MBOs, NLMOBOs, $\nabla^2\rho_{BCP}$, FOPs, and BDEs of Some Hydrocarbons

molecule	bond	LBO	MBO	NLMOBO	$\nabla^2\rho_{BCP}$	FOP	BDE[b]
ethane	C−C	1.007	1.121	1.025	−0.515	0.309	368
	C−H	0.957	0.975	0.777	−0.926	0.121	410
ethene	C−C	1.901	2.126	2.026	−0.869	0.392	682
	C−H	0.988	0.953	0.780	−1.001	0.123	427
acetylene	C−C	2.557	2.707	3.007	−0.977	0.461	962
	C−H	1.003	1.038	0.757	−1.129	0.125	523
benzene	C−C	1.466	1.463	1.713/1.288[a]	−0.737	0.311	
	C−H	0.977	0.942	0.752	−1.012	0.113	
cyclopropane	C−C	0.724	1.040	1.040	−0.379	0.239	
	C−H	0.968	0.961	0.764	−0.982	0.118	423

[a]The two values appear alternately in the 6-MR ring. [b]BDEs.

covalent radii should be modified before applying them directly to construct the Becke's overlap space. The main reason for this is that the main group elements with small (large) covalent radii generally have large (small) electronegativity and thus prefer to withdraw (donate) electrons to expand (shrink) their effective sizes in a molecule environment. Due to these behaviors, the actual radii of main group elements in each row tend to be equalized. On the basis of this observation, we decide to replace covalent radii of main group elements (except for H and He) with those of IVA group elements in the same row. For most cases, as discussed below, this modification makes the overlap space much closer to the valence electron bonding region.

It is worthy to note that the fuzzy overlap space concept in some sense can be regarded as an extension of the AIM topology analysis methodology.[23] In AIM theory, an interatomic interaction is commonly characterized by real space properties such as ρ, $\nabla^2\rho$, the potential energy density,[23] and the kinetic energy density[23] at the corresponding bond critical point (BCP),[34] which has a vanishing total gradient of ρ and possesses two negative and one positive eigenvalue of the Hessian of ρ. The sign of $\nabla^2\rho$ at BCP (referred to as $\nabla^2\rho_{BCP}$ later) is a generally recognized criterion for discriminating bond types.[35] Negative and positive signs suggest that the bond is formed by covalent and closed-shell interactions, respectively. However, only taking the BCP into account is sometimes not enough to determine the nature of the bond of interest. Irrational position of the BCP and neglect of the surrounding environment of the BCP tend to result in erroneous conclusions.[35] The C−O bond shown in Figure 1 is just one such case. The blue points in the figure are BCPs. It is well-known that the C−O bond is a typical polar covalent bond; however, the corresponding BCP presents in the positive region of $\nabla^2\rho$; therefore, the sign of $\nabla^2\rho_{BCP}$ erroneously indicates that the C−O bond stems from a closed-shell interaction. On the other hand, LBO characterizes the $\nabla^2\rho$ in the whole bonding region; hence, it can be expected that the LBO would be more reliable, as will be shown later.

It should be emphasized that the LBO is a definition of covalent bond order rather than total bond order. Noncovalent interactions thus have no contribution to the LBO. This feature of LBO is analogous to NLMOBO, which also only reflects covalency[11] but was defined in Hilbert space, namely, natural atomic orbital basis.[36]

3. COMPUTATIONAL AND TECHNICAL DETAILS

Electronic wave functions of all test molecules were generated by the Gaussian 03 package.[37] Unless otherwise specified, the B3LYP hybrid functional[38] with the cc-pVDZ basis-set[39] was used. All molecular geometrics were optimized at this level. When transition metals were involved, the second-order Douglas−Kroll−Hess (DKH) method[40−43] was utilized to take scalar relativistic effects into account; meanwhile the basis set was replaced with cc-pVDZ-DK,[44] which is a recontracted version of cc-pVDZ specific for the DKH Hamiltonian. In practical applications of the LBO, such an expensive full-electron scalar relativistic calculation is generally unnecessary, and we found that the results can be well-reproduced by the calculations using small-core relativistic pseudopotentials, for example, cc-pVDZ-PP.[45] NLMOBOs were computed by the NBO 3.1 module of the Gaussian 03 package. LBOs, $\nabla^2\rho_{BCP}$, FOPs, and MBOs were all calculated by Multiwfn 2.6.1,[46] which is a multifunctional wave function analysis program developed by us that can be freely downloaded.[47] Becke's atomic weighting function with $k = 3$ was used for both the LBO and FOP.

The covalent radii deduced from crystallographic data[30] were employed. For main group elements, the radii were modified as mentioned in the last section. The bond dissociation energy (BDE) data were taken from ref 48; the units are in kJ/mol.

The integration involved in the LBO can be readily evaluated by Becke's multicenter numerical integration scheme.[19] The second kind of Gauss−Chebyshev[49] and Lebedev−Laikov[50] methods are employed for integrating radial and angular parts, respectively. In the Supporting Information, we examined the dependence of the LBO on the quality of the integration grid. We found that even at a very coarse grid level, for example, 30 radial points in combination with 110 Lebedev−Laikov angular points, the result is still accurate. In this situation, the computation amount for evaluating the LBO is always negligible relative to that for yielding the electronic wave function. However, in order to minimize the error of the LBO due to integration accuracy, the LBO values as well as the FOP values presented below were all calculated with 75 radial points and 434 angular points.

4. RESULTS AND DISCUSSIONS

In this section, we systematically examine the LBO through a wide variety of molecules. Meanwhile, the LBO will be compared with the aforementioned NLMOBO, FOP, $\nabla^2\rho_{BCP}$, as well as MBO, which may be the most prevalently used bond order nowadays.

The BDE is a measure of the bond strength. As a quantitative description of chemical bonds, the bond order should have some sort of a correlation with the BDE. This point was mentioned by Politzer.[4−6] Therefore, in this section, the BDE

dx.doi.org/10.1021/jp4010345 | J. Phys. Chem. A 2013, 117, 3100−3108

Table 2. Experimental Vibrational Frequencies[9] (cm^{-1}), LBOs, MBOs, NLMOBOs, $\nabla^2\rho_{BCP}$, and FOPs of the C−O Bond in Carbon Monoxide and in Different Metal Carbonyl Complexes

molecules	frequency	LBO	MBO	NLMOBO	$\nabla^2\rho_{BCP}$	FOP
CO	2143	1.882	2.621	1.515	1.805	0.434
$Cu(CO)^+$	2230	1.974	2.676	1.717	1.971	0.409
$Ni(CO)_4$	2060	1.738	2.488	1.558	1.529	0.408
$Cr(CO)_6$	2000	1.681	2.369	1.554	1.457	0.400
$Co(CO)_4^-$	1890	1.495	2.292	1.449	1.173	0.402
$Sc(CO)^-$	1732	1.287	2.142	1.294	1.029	0.392
adj. R^{2a}		0.996	0.971	0.819	0.956	0.352

[a]Adjusted R^2 yielded by a linear fitting of the corresponding quantities to the vibrational frequencies.

Table 3. LBOs, MBOs, NLMOBOs, $\nabla^2\rho_{BCP}$, and FOPs for a Variety of Diatomic and Polyatomic Molecules

molecule	bond	LBO	MBO	NLMOBO	$\nabla^2\rho_{BCP}$	FOP
H_2	H−H	0.964	1.000	1.000	−1.217	0.126
Li_2	Li−Li	0.355	1.007	1.000	−0.013	0.164
Na_2	Na−Na	0.096	0.991	1.001	−0.002	0.158
N_2	N−N	3.046	2.928	3.012	−2.022	0.464
P_2	P−P	1.860	2.948	3.004	−0.332	0.498
B_2[a]	B−B	1.014	2.354	2.604	−0.181	0.302
C_2	C−C	1.648	3.512	3.701	−0.283	0.424
C_{60}	C−C [5,6][c]	1.116	1.182	*d*	−0.610	0.238
thiophene	C−C [6,6][c]	1.365	1.388	*d*	−0.712	0.267
	$S-C_\alpha$	0.913	1.192	1.067	−0.416	0.298
	$C_\alpha-C_\beta$	1.528	1.628	1.753	−0.750	0.310
	$C_\beta-C_\beta$	1.278	1.303	1.215	−0.656	0.287
ClF_3	$Cl-F_{Axial}$	0.089	0.769	0.501	0.248	0.279
	$Cl-F_{Equat.}$	0.104	0.885	0.682	0.093	0.285
CO_2	C−O	1.395	2.254	1.470/1.293	0.833	0.402
borazine	B−N	0.781	1.364	0.651/0.626[e]	0.727	0.285
Ne_2[b]	Ne−Ne	0.000	0.000	0.000	0.016	0.019
HCN	C−N	2.676	3.155	2.675	0.666	0.460
	C−H	0.992	0.970	0.762	−1.152	0.121
NO	N−O	1.488	2.261	1.808	−1.969	0.424
NO^+	N−O	2.698	2.748	2.209	−3.219	0.433
CH_3CHO	C−O	0.938	2.226	1.396	0.671	0.398
	C−C	1.115	1.055	0.980	−0.578	0.284
PCl_3	P−Cl	0.396	1.067	0.701	−0.113	0.309
SiH_4	Si−H	0.824	0.961	0.848	0.281	0.144
$COCl_2$	C−O	1.373	2.281	1.412	1.087	0.366
	C−Cl	0.517	1.027	0.931	−0.240	0.251
NH_3BF_3	N−H	0.863	0.975	0.571	−1.529	0.111
	B−F	0.064	1.239	0.418	0.213	0.171
	N−B	0.196	0.674	0.272	1.074	0.247
LiF	Li−F	0.033	0.979	0.192	0.728	0.206
NaCl	Na−Cl	0.143	0.855	0.165	0.205	0.239

[a]B_2 is the triplet in the ground state. [b]An equilibrium distance of 3.1007 Å[52] was used. [c]C−C [5,6] stands for the C−C bond shared by five-member and six-member rings, and C−C [6,6] is that shared by two six-member rings. [d]The NBO 3.1 program is not supported for such a large system. [e]The two quantities occur alternately in the ring.

as well as the bond vibrational frequency will be exploited as two important indices to demonstrate the quality of different bond order definitions.

Hydrocarbons. LBOs, MBOs, NLMOBOs, $\nabla^2\rho_{BCP}$, and FOPs of some typical hydrocarbons are given in Table 1. BDEs are listed in the last column of the table. For the C−C bond in ethane, ethene, and acetylene, it is clear that the bond multiplicities can be well discriminated by LBO, MBO, and NLMOBO. NLMOBOs are almost exactly equal to the formal bond orders. However, the relative ratio 1:1.96:2.56 (1:1.90:2.41) of the LBOs (MBOs) of C−C bonds in ethane, ethene, and acetylene is in agreement with the ratio 1:1.85:2.61 of the BDEs of the C−C bonds in these molecules, which indicates that LBOs and MBOs have a better correlation with BDEs than NLMOBOs, whose corresponding ratio is 1:1.97:2.93. For C−C bonds in benzene, LBOs and MBOs are nearly identical; the value of 1.46 is quite reasonable because the bond can formally be considered as a typical σ bond plus a half of a π bond. NLMOBOs of C−C bonds in benzene vary alternately between 1.713 and 1.288 and hence failed to exhibit the equalization characteristic of electrons due to six-center delocalization. The root of this problem is mainly

dx.doi.org/10.1021/jp4010345 | J. Phys. Chem. A 2013, 117, 3100−3108

due to the fact that the definition of NLMOBO is based on the localized molecular orbital representation. LBOs of C−C bonds in cyclopropane are noticeably smaller than that in ethane, correctly reflecting the fact that the bonds are weakened by the strong strain effect, whereas this effect is only marginally revealed by MBO and not by NLMOBO at all.

For all C−H bonds in Table 1, LBOs and MBOs are close to the formal bond order (1.0), while NLMOBOs somewhat underestimates of the bond orders. Among these three bond order definitions, only the LBO correctly reproduced the BDE sequence of the C−H bond in ethane, ethene, and acetylene, as shown in the last column in Table 1.

The changing trend of $\nabla^2\rho_{BCP}$ and FOPs of C−C bonds in Table 1 are basically consistent with the LBO. However, $\nabla^2\rho_{BCP}$ and FOP are evidently inappropriate to be regarded as bond order, even after scaling in some ways. First, they cannot adequately discriminate bond multiplicities. For instance, the magnitude of $\nabla^2\rho_{BCP}$ of the triple C−C bond (−0.977) is just slightly larger than that of the double C−C bond (−0.869), while the difference between the FOPs of the C−C bonds in ethane and benzene is even as small at 0.002. Second, the magnitudes of FOP and $\nabla^2\rho_{BCP}$ for different types of bonds are not comparable. For example, the FOP of the C−C bond (0.309) in ethane is more than twice of that of the C−H bond (0.121), while the magnitude of $\nabla^2\rho_{BCP}$ of the C−C bond (−0.515) is only about half of that of the C−H bond (−0.926), although both the C−C and C−H bonds have almost the same formal bond order (1.0).

Carbon Monoxide and Metal Carbonyl Complexes. Bond orders, $\nabla^2\rho_{BCP}$, and FOPs of the C−O bond in carbon monoxide and in some metal carbonyl complexes are calculated and then linearly fitted to C−O experimental vibrational frequencies,[9] which directly relate to the bond strength like the BDEs.[51] The results are presented in Table 2. From adjusted R^2 values, one can see that both LBO and MBO have a very good linear correlation with vibrational frequencies, and the former performs even better, the adjusted R^2 strikingly reached 0.996. This is consistent with the conclusion drawn for hydrocarbon molecules in the last subsection. NLMOBO has worse correlation with vibrational frequencies. It can be seen from the table that the relative strength of the C−O bond in $Co(CO)_4^-$ and in $Cr(CO)_6$ is not properly reflected by FOP. Moreover, FOP overestimated the C−O bond strength in the CO molecule. Therefore, it is not reliable to compare a bond in different chemical environments by using FOP. Values of $\nabla^2\rho_{BCP}$ are listed in the sixth column of the table. Although the linear correlation of $\nabla^2\rho_{BCP}$ with the vibrational frequencies is better than NLMOBO and FOP, yet the sign of $\nabla^2\rho_{BCP}$ is not negative as expected and thus exhibits a wrong nature of the C−O bond.

Variety of Diatomic and Polyatomic Molecules. Calculated bond orders, $\nabla^2\rho_{BCP}$, and FOPs for a number of structurally diverse molecules are listed in Table 3. We first consider diatomic molecules in the upper part of the table. LBO, MBO, and NLMOBO are almost the same for the typical covalent systems, that is, H_2 and N_2, although their theoretical bases are quite different. The BDE sequences (values in kcal/mol given in parentheses) $H_2(436) > Li_2(106) > Na_2(77)$ and $N_2(945) > P_2(490)$ are well reproduced by LBO. However, contrary to the results in Tables 1 and 2, MBO fails to show the correct order of these BDE sequences. As discussed before, NLMOBO also does not show any direct correlation with the BDE for these molecules. The LBO values of B_2 and C_2 are 1.014 and 1.648, respectively. They are much lower than the corresponding MBO and NLMOBO values in the table. However, in comparison with the LBO value of 1.007 for the C−C single bond in ethane, these LBO values for B_2 and C_2 are reasonable because BDEs of B_2 and C_2 are just 0.81 and 1.65 times the BDE of the C−C single bond in ethane listed in Table 1, respectively.

Next, we discuss the results of fullerene, thiophene, and ClF_3 near the middle of the table. Within these three molecules, there are two types of bonds each: the bond fusing two six-member rings (6-MR) and the one fusing one 5-MR and one 6-MR in the fullerene; the bond linking an α and a β carbon and the one linking two β carbons in thiophene; and the bond between Cl and the equatorial F and the one between Cl and the axial F in ClF_3. The length of the former type of bonds is shorter than that of the latter. For these three molecules, all values of the LBO, MBO, and NLMOBO are consistent with the bond length changes, which are related to bond strengths.

The above results as well as those in Tables 1 and 2 indicate that the LBO has a strong correlation with the bond strength. Although this is in general not true for them, MBO and NLMOBO can still be used to show the relative strengths of the same type of bonds within a molecule, such as in the fullerene, thiophene, and ClF_3.

As discussed before for benzene in Table 1, owing to the presence of conspicuous three-center delocalization in CO_2[53] and very weak six-center delocalization in borazine,[54] NLMOBOs of CO_2 and borazine listed in the middle of Table 3 are not in accordance with molecular symmetries because this bond order definition is always prone to exhibit a localized bonding pattern. Because of this, NLMOBO is not suitable for conjugated systems. Another noteworthy issue is that the NLMOBO values between nonadjacent atoms are usually not negligible and sometimes even negative. For example, the NLMOBO between methyl carbon and oxygen in CH_3CHO is −0.063, which obviously lacks a physical meaning. These problems of the NLMOBO do not exist in the LBO and MBO.

As expected, all three bond orders of the Ne_2 dimer are zero because the Ne_2 dimer is bounded by the dispersion effect rather than a chemical bond. FOP seems to be useless for comparing chemical bonds with different constituent elements. For example, it absurdly indicates that the Li_2 is more strongly bonded than H_2.

For all polar bonds in Table 3, the LBO and NLMOBO are obviously smaller than the MBO in different degrees. This common feature again shows that the LBO and NLMOBO mainly reflect the covalent bond order other than the total bond order. Because of the extremely high polarity, the LBO of the B−F bond in NH_3BF_3 is even close to zero (its corresponding $\nabla^2\rho$ map was plotted as Figure S4, Supporting Information). LBOs of Cl−F bonds in ClF_3 are also quite small, but this is not because of the bond polarity. From the $\nabla^2\rho$ map, the electron deformation map, and the electron localization function[55,56] map of ClF_3 (Figures S4−S6, respectively, Supporting Information), neither prominent electron concentration nor electron accumulation nor electron localization in the bonding region can be observed. These phenomena are the consequences that the nature of Cl−F bonds are typical charge-shift bonds.[57]

Because LiF is an ionic compound, the LBO is almost zero, as expected. Although NaCl has similar or even stronger ionic characteristic than LiF, the LBO for NaCl is larger than that of

dx.doi.org/10.1021/jp4010345 | J. Phys. Chem. A 2013, 117, 3100−3108

LiF. This abnormal behavior implies that LBO at the present stage may not be robust for ionic bonds. We found that this issue could be hopefully resolved by employing a more reasonable and thus more complicated atomic weighting function. A detailed discussion about this point is given in section 4 of the Supporting Information.

The necessity of modifying atomic radii before calculating the LBO, as was emphasized in section 2, is demonstrated in Table S3 (Supporting Information). From the table, it can be seen that for most of the bonds involved in Table 3, the modification of atomic radii does not much alter the LBO values. However, for the highly polar bonds, if the original atomic radii are used, then the LBO result will be unreasonable. For instance, in NH_3BF_3, the LBO of the B−F bond (0.362) will be larger than that of the B−N bond (0.326), which contradicts the truth that the B−F bond has higher polarity than the B−N bond. Although the LBO at the present stage is not very suitable for ionic bonds, if the atomic radii remain unmodified, then the LBO will be completely meaningless for this type of bond, for example, LiF and NaCl will have LBO values of 1.027 and 0.841.

We also studied the bond orders of 1,3$\lambda^4\delta^2$,2,4-benzodithiadiazine, which is a more complex molecule and has been deeply studied by Oláh and co-workers.[25] The computed LBO values are in good agreement with their results.[25] The data are presented in section 6 of the Supporting Information.

Methane Substitution Effects. The LBO, MBO, NLMOBO, FOP, and $\nabla^2\rho_{BCP}$ of the C−X bond in CH_3XH_n (X = C, N, O, F; n = 0, 1, 2, 3) are shown in Figure 3. Because

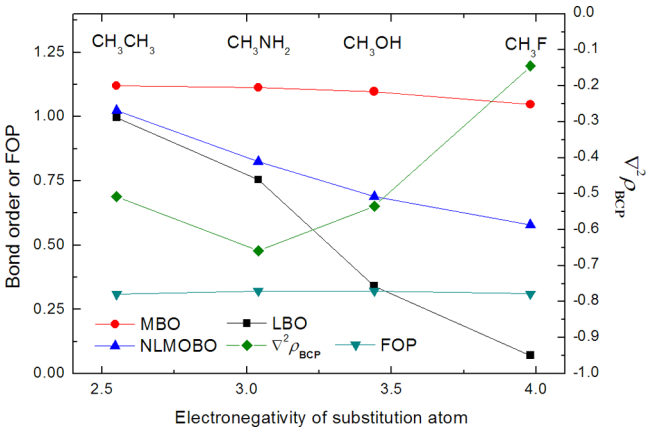

Figure 3. Variations of the LBO, MBO, NLMOBO, FOP, and $\nabla^2\rho_{BCP}$ of the C−X bond in CH_3XH_n (X = C, N, O, F) with respect to the electronegativity of the substitution atom X.

the LBO and NLMOBO only reflect covalency, they almost decrease linearly with the increase of polarity of the C−X bond, as expected. The slope of the former is larger than that of the latter, showing that the LBO is more sensitive to bond polarity than the NLMOBO. The MBO is almost unaffected by bond polarity; thus, to some extent, the MBO can be regarded as a measure of the total bond order. Interestingly, the bond polarity also has no influence on the FOP. This may be just a coincidence in the present test. Although $\nabla^2\rho_{BCP}$ is also a quantity reflecting charge concentration in the bonding region like the LBO, no clear relationship between $\nabla^2\rho_{BCP}$ and the bond polarity can be seen from Figure 3. This observation implies that only extracting information from one point (BCP) is not enough to study bond properties, and the entire bonding region (fuzzy overlap space) should be taken into account.

Conformational Isomerization of 1,3-Butadiene. In order to study the variations of bond orders with geometrical changes, we calculate the bond orders of 1,3-butadiene. Two C−C double bonds in 1,3-butadiene rotate around the C2−C3 bond, driving the geometry changes from the cis structure to the trans structure. The bond orders are plotted as Figure 4. It

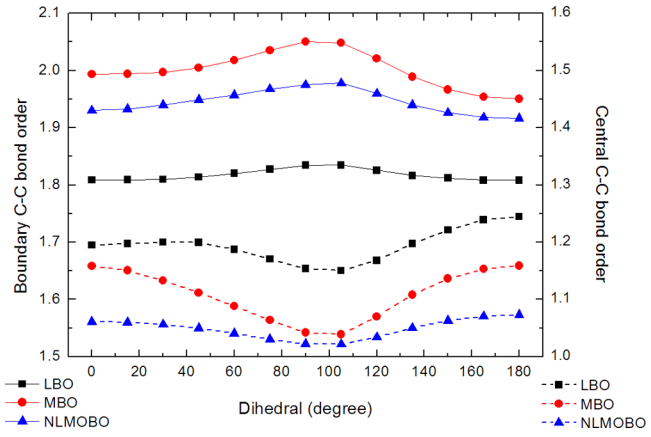

Figure 4. The variations of the LBO, MBO, and NLMOBO of the central and boundary C−C bonds of 1,3-butadiene with respect to torsion of its C−C−C−C dihedral angle. The 0 and 180° correspond to the cis and trans conformations, respectively. All other geometrical variables are free to relax.

is well-known that the π-conjugate in boundary C−C bonds is significantly stronger than that in the central C−C bond; thus, the boundary C−C bond should have larger bond order than the central C−C bond. Besides, it is expected that the bond order of the central C−C (the boundary C−C) should have a minimum (maximum) at the dihedral angle of 90°, owing to the maximal break of the π-conjugate along the carbon chain. From the figure, it can be seen clearly that all LBOs, MBOs, and NLMOBOs are in perfect agreement with the above expectations. In addition, due to sterical effects, the central C−C bond length in the cis conformation is slightly longer than that in the trans conformation. This effect is faithfully reflected in Figure 4 by the LBO and NLMOBO. However, the difference of the MBO of the central C−C bond between the cis and trans conformations is just 0.001, which is too small to reflect the steric effect.

Dissociation Curve of N_2. The variations of the LBO, MBO, NLMOBO, FOP, and $\nabla^2\rho_{BCP}$ of the N−N bond in N_2 with the bond length are presented in Figure 5. In order to describe the dissociation behavior of N_2 properly, the broken-symmetry method[58] was used in the calculation. The optimized equilibrium bond length is 1.104 Å. As shown in Figure 5, the curves of the LBO, MBO, NLMOBO, FOP, and $\nabla^2\rho_{BCP}$ start from the equilibrium position and end at r_{N-N} = 2.2 Å.

As the N−N bond length becomes large, the LBO decreases smoothly and shows correct dissociation behavior. The dissociation curve was fitted to an exponential function as follows

$$\mathrm{LBO}(\mathbf{r}) = 3.2 \times \exp[-4.63(\mathbf{r} - \mathbf{r}_0)] \quad (6)$$

The adjusted R^2 of the above fitting is as high as 0.997. We surprisingly noted that this equation is in perfect accord with

dx.doi.org/10.1021/jp4010345 | J. Phys. Chem. A 2013, 117, 3100−3108

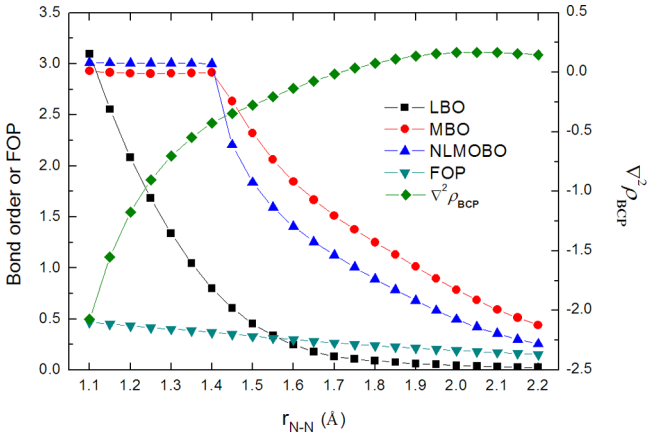

Figure 5. The variations of the LBO, MBO, NLMOBO, FOP, and $\nabla^2\rho_{BCP}$ of the N−N bond in N_2 along the dissociation curve. The optimized equilibrium bond length is 1.104 Å.

the Pauling's well-known bond order−bond length exponential relationship.[59]

The increase of $\nabla^2\rho_{BCP}$ and the decrease of the LBO are synchronized, and their variations can be considered as rendering the same physical picture. The convergence of the FOP to zero is quite slow, and the variation trend is basically a straight line, which can be fitted as $\mathrm{FOP}(\mathbf{r}) = 0.454 \times (\mathbf{r} - \mathbf{r}_0) - 0.292$ with the adjusted R^2 as 0.990.

The MBO and NLMOBO have similar dissociation behaviors. As can be seen from Figure 5, there is along the MBO and NLMOBO curves an instablilty point where the restricted and unrestricted B3LYP descriptions start to differ. In the present case, the position of the instability point is around 1.40 Å. Both the MBO and NLMOBO remain almost constant within the r_{N-N} interval [1.104, 1.40] and begin to decrease only beyond the instablity point. This indicates that the MBO and NLMOBO are unable to predict qualitatively the variation of bond strength before the instablity point.

Dependences on Theoretical Methods and Basis Sets. First, we employed formamide as a test molecule to examine the dependence of the LBO on theoretical methods. Results are shown in Figure 6. The HF method,[60] two popular post-HF methods MP2 and CCSD,[60] a local density approximation (LDA) functional SVWN3,[61,62] a generalized gradient approximation functional PBE,[63] and two representative hybrid functionals PBE0[64] and B3LYP were taken into consideration. One can see from the figure that LBOs of N−H, C−N, C−H, and C−O in formamide decrease significantly as the theoretical method changes from HF to other correlation methods, which indicates that the electron correlation effect has a notable impact on the LBO. However, LBO becomes rather insensitive to all correlation methods. Reasonable results can be obtained even at LDA level. As shown in Figure 6, the LBOs produced with B3LYP and PBE0 densities are very close to the ones produced under high-quality CCSD density.

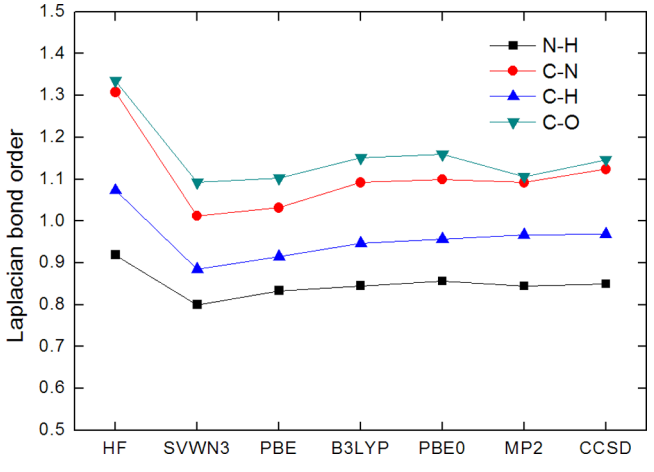

Figure 6. The variation of LBOs of bonds in formamide with respect to theoretical methods. The basis set is cc-pVDZ. The geometry was optimized at the B3LYP/cc-pVDZ level.

Basis set dependency of the LBO was also examined with formamide. As shown in Figure 7, LBOs of N−H, C−N, C−H, and C−O have some variations as the basis set goes from STO-3G, to 3-21G, to 6-31G. However, as the basis set changes to the middle- and higher-quality ones like cc-pVDZ and beyond, the sensitivity of the LBO becomes low. Moreover, diffusion functions such as those in aug-cc-pVDZ and aug-cc-pVTZ have almost undetectable influences on the LBO in comparison with the results obtained with cc-pVDZ and cc-pVTZ. Therefore, cc-pVDZ or a similar quality of basis sets will be an optimal choice for large systems for evaluating the LBO.

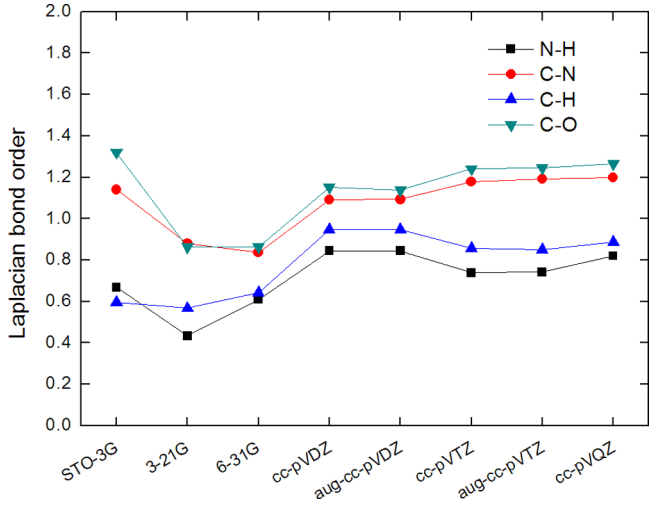

Figure 7. The variation of the LBO of bonds in formamide with respect to the basis set. B3LYP is employed as a theoretical method. The geometry was optimized at the B3LYP/cc-pVDZ level.

5. CONCLUSIONS

In this paper, we present a novel covalent bond order definition named the Laplacian bond order (LBO), which is based on integrating negative parts of the Laplacian of the electron density in fuzzy overlap space. Its reasonableness and usefulness are demonstrated by applying it to a wide variety of molecules and by comparing it with the Mayer bond order (MBO) and natural localized molecular orbital bond order (NLMOBO). The LBO has a better ability to discriminate bonding strength than the MBO and NLMOBO and has a direct correlation with bond polarity, BDE, and bond vibrational frequency. The computational cost of the LBO is low. Satisfactory results can be obtained even at the B3LYP/cc-pVDZ level. This means that the LBO can be applied to rather large systems. Because the LBO is inherently independent of the wave function, one can, in principle, obtain the LBO by making use of accurate

dx.doi.org/10.1021/jp4010345 | J. Phys. Chem. A 2013, 117, 3100−3108

electron densities derived from X-ray diffraction data. We believe that the LBO proposed herein could be a very useful tool for chemists to analyze the electronic structure characteristics of molecules or even infinite extended systems.

In present study, we also found that the fuzzy overlap population (FOP), namely, the integral of the electron density in fuzzy overlap space, is inappropriate to use as a measure of bond order. Electron density at the bond critical point $\nabla^2\rho_{BCP}$ has been discussed in a larger number of literature reports. In some sense, the LBO can be viewed as an extension of $\nabla^2\rho_{BCP}$ from a sole critical bond point to the whole bonding region. It is clear from our present studies that the LBO has remarkable advantages over $\nabla^2\rho_{BCP}$ in measuring the strength and polarity of bonds.

Currently, the LBO is for the bond order of two centers. However, its extension to multicenter cases is straightforward. Integrations of the fuzzy overlap space over the energy density,[23] ELF, source function,[65] deformation density, and Fermi hole[66] are also of interest. In addition, in the current definition of the LBO, we only take the negative part of $\nabla^2\rho$ into account, while the positive part of which may be also valuable and thus should not be simply ignored; for example, its integration value perhaps has some close relations with the noncovalent interaction strength. These directions will be lines of our future research, which may further expand the application range of the LBO and enrich the uses of fuzzy overlap space analysis.

■ ASSOCIATED CONTENT

Supporting Information

Definition of the fuzzy atom and illustration of fuzzy overlap space. Plane graphs of some molecules involved in the main text. Discussion of the dependence of the Laplacian bond order on the numerical integration grid and the ways to improve the Laplacian bond order for ionic bonds. The influence of modification of atomic radii on the LBO values. Comparison of bond orders for 1,3$\lambda^4\delta^2$,2,4-benzodithiadiazine. This material is available free of charge via the Internet at http://pubs.acs.org.

■ AUTHOR INFORMATION

Corresponding Author

*E-mail: chenfeiwu@ustb.edu.cn.

Notes

The authors declare no competing financial interest.

■ ACKNOWLEDGMENTS

The authors thank the National Natural Science Foundation of China (Project No. 21173020) for the financial support.

■ REFERENCES

(1) Coulson, C. A. The Electronic Structure of Some Polyenes and Aromatic Molecules. VII. Bonds of Fractional Order by the Molecular Orbital Method. *Proc. R. Soc. London, Ser. A* **1939**, *169*, 413−428.
(2) Wiberg, K. B. Application of the Pople−Santry−Segal CNDO Method to the Cyclopropylcarbinyl and Cyclobutyl Cation and to Bicyclobutane. *Tetrahedron* **1968**, *24*, 1083−1096.
(3) Mayer, I. Charge, Bond Order and Valence in the Ab Initio SCF Theory. *Chem. Phys. Lett.* **1983**, *97*, 270−274.
(4) Politzer, P. Bond Orders of Heteronuclear Diatomic Molecules. *J. Chem. Phys.* **1969**, *51*, 459−460.
(5) Politzer, P. Bond Orders of Homonuclear Diatomic Molecules. *J. Chem. Phys.* **1969**, *50*, 2780−2781.
(6) Politzer, P.; Ranganathan, S. Bond-Order−Bond-Energy Correlations. *Chem. Phys. Lett.* **1986**, *124*, 527−530.
(7) Cioslowski, J.; Mixon, S. T. Covalent Bond Orders in the Topological Theory of Atoms in Molecules. *J. Am. Chem. Soc.* **1991**, *113*, 4142−4145.
(8) Glendening, E. D.; Weinhold, F. Natural Resonance Theory: II. Natural Bond Order and Valency. *J. Comput. Chem.* **1998**, *19*, 610−627.
(9) Michalak, A.; DeKock, R. L.; Ziegler, T. Bond Multiplicity in Transition-Metal Complexes: Applications of Two-Electron Valence Indices. *J. Phys. Chem. A* **2008**, *112*, 7256−7263.
(10) Roos, B. O.; Borin, A. C.; Gagliardi, L. Reaching the Maximum Multiplicity of the Covalent Chemical Bond. *Angew. Chem.* **2007**, *119*, 1491−1494.
(11) Reed, A. E.; Schleyer, P. v. R. Chemical Bonding in Hypervalent Molecules. The Dominance of Ionic Bonding and Negative Hyperconjugation over d-Orbital Participation. *J. Am. Chem. Soc.* **1990**, *112*, 1434−1445.
(12) Fradera, X.; Austen, M. A.; Bader, R. F. W. The Lewis Model and Beyond. *J. Phys. Chem. A* **1998**, *103*, 304−314.
(13) Bader, R. F. W.; Stephens, M. E. Spatial Localization of the Electronic Pair and Number Distributions in Molecules. *J. Am. Chem. Soc.* **1975**, *97*, 7391−7399.
(14) Matito, E.; Poater, J.; Solà, M.; Duran, M.; Salvador, P. Comparison of the AIM Delocalization Index and the Mayer and Fuzzy Atom Bond Orders. *J. Phys. Chem. A* **2005**, *109*, 9904−9910.
(15) Mayer, I.; Salvador, P. Overlap Populations, Bond Orders and Valences for 'Fuzzy' Atoms. *Chem. Phys. Lett.* **2004**, *383*, 368−375.
(16) Jules, J. L.; Lombardi, J. R. Toward an Experimental Bond Order. *J. Mol. Struct.: THEOCHEM* **2003**, *664−665*, 255−271.
(17) Gross, L.; Mohn, F.; Moll, N.; Schuler, B.; Criado, A.; Guitián, E.; Peña, D.; Gourdon, A.; et al. Bond-Order Discrimination by Atomic Force Microscopy. *Science* **2012**, *337*, 1326−1329.
(18) Hirshfeld, F. L. Bonded-Atom Fragments for Describing Molecular Charge Densities. *Theor. Chem. Acc.* **1977**, *44*, 129−138.
(19) Becke, A. D. A Multicenter Numerical Integration Scheme for Polyatomic Molecules. *J. Chem. Phys.* **1988**, *88*, 2547−2553.
(20) Lu, T.; Chen, F. Comparison of Computational Methods for Atomic Charges. *Acta Phys. Chim. Sin.* **2012**, *28*, 1−18.
(21) Lu, T.; Chen, F. Atomic Dipole Moment Corrected Hirshfeld Population Method. *J. Theor. Comput. Chem.* **2012**, *11*, 163−183.
(22) Lu, T.; Chen, F. Calculation of Molecular Orbital Composition. *Acta Chim. Sin.* **2011**, *69*, 2393−2406.
(23) Bader, F. W. *Atoms in Molecules: A Quantum Theory*; Oxford University Press: New York, 1994.
(24) Rousseau, B.; Peeters, A.; Alsenoy, C. V. Atomic Charges from Modified Voronoi Polyhedra. *J. Mol. Struct.: THEOCHEM* **2001**, *538*, 235−238.
(25) Oláh, J.; Blockhuys, F.; Veszprémi, T.; Van Alsenoy, C. On the Usefulness of Bond Orders and Overlap Populations to Chalcogen−Nitrogen Systems. *Eur. J. Inorg. Chem.* **2006**, *2006*, 69−77.
(26) Gillespie, R. J.; Popelier, P. L. A. *Chemical Bonding and Molecular Geometry—From Lewis to Electron Densities*; Oxford University Press: New York, 2001; pp 163−180.
(27) Shi, Z.; Boyd, R. J. The Shell Structure of Atoms and the Laplacian of the Charge Density. *J. Chem. Phys.* **1988**, *88*, 4375−4377.
(28) Shi, Z.; Boyd, R. J. The Laplacian of the Charge Density as a Probe of Reaction Paths and Reactivity: A Comparison of S_N2 Reactions at Carbon and Silicon. *J. Phys. Chem.* **1991**, *95*, 4698−4701.
(29) Lillestolen, T. C.; Wheatley, R. J. Redefining the Atom: Atomic Charge Densities Produced by an Iterative Stockholder Approach. *Chem. Commun.* **2008**, 5909−5911.
(30) Cordero, B.; Gomez, V.; Platero-Prats, A. E.; Reves, M.; Echeverria, J.; Cremades, E.; Barragan, F.; Alvarez, S. Covalent Radii Revisited. *Dalton Trans.* **2008**, 2832−2838.
(31) Pyykkö, P.; Atsumi, M. Molecular Single-Bond Covalent Radii for Elements 1−118. *Chem.—Eur. J.* **2009**, *15*, 186−197.
(32) Suresh, C. H.; Koga, N. A Consistent Approach toward Atomic Radii. *J. Phys. Chem. A* **2001**, *105*, 5940−5944.

(33) Boyd, R. J. The Relative Sizes of Atoms. *J. Phys. B: At. Mol. Phys.* **1977**, *10*, 2283−2291.
(34) Bianchi, R.; Gervasio, G.; Marabello, D. Experimental Electron Density Analysis of $Mn_2(CO)_{10}$: Metal−Metal and Metal−Ligand Bond Characterization. *Inorg. Chem.* **2000**, *39*, 2360−2366.
(35) Stalke, D. Meaningful Structural Descriptors from Charge Density. *Chem.—Eur. J.* **2011**, *17*, 9264−9278.
(36) Reed, A. E.; Weinhold, F. Natural Bond Orbital Analysis of Near-Hartree—Fock Water Dimer. *J. Chem. Phys.* **1983**, *78*, 4066−4073.
(37) Frisch, M. J.; Trucks, G. W.; Schlegel, H. B.; Scuseria, G. E.; Robb, M. A.; Cheeseman, J. R.; Montgomery, J. A., Jr.; Vrevon, T.; et al. *Gaussian 03*, version E.01; Gaussian, Inc.: Wallingford, CT, 2004.
(38) Becke, A. D. A New Mixing of Hartree—Fock and Local Density-Functional Theories. *J. Chem. Phys.* **1993**, *98*, 1372−1377.
(39) Dunning, J. T. H. Gaussian Basis Sets for Use in Correlated Molecular Calculations. I. The Atoms Boron through Neon and Hydrogen. *J. Chem. Phys.* **1989**, *90*, 1007−1023.
(40) Douglas, M.; Kroll, N. M. Quantum Electrodynamical Corrections to the Fine Structure of Helium. *Ann. Phys.* **1974**, *82*, 89−155.
(41) Hess, B. A. Applicability of the No-Pair Equation with Free-Particle Projection Operators to Atomic and Molecular Structure Calculations. *Phys. Rev. A* **1985**, *32*, 756−763.
(42) Hess, B. A. Relativistic Electronic-Structure Calculations Employing a Two-Component No-Pair Formalism with External-Field Projection Operators. *Phys. Rev. A* **1986**, *33*, 3742−3748.
(43) Jansen, G.; Hess, B. A. Revision of the Douglas−Kroll Transformation. *Phys. Rev. A* **1989**, *39*, 6016−6017.
(44) de Jong, W. A.; Harrison, R. J.; Dixon, D. A. Parallel Douglas−Kroll Energy and Gradients in NWChem: Estimating Scalar Relativistic Effects Using Douglas−Kroll Contracted Basis Sets. *J. Chem. Phys.* **2001**, *114*, 48−53.
(45) Peterson, K. A.; Puzzarini, C. Systematically Convergent Basis Sets for Transition Metals. II. Pseudopotential-Based Correlation Consistent Basis Sets for the Group 11 (Cu, Ag, Au) and 12 (Zn, Cd, Hg) Elements. *Theor. Chem. Acc.* **2005**, *114*, 283−296.
(46) Lu, T.; Chen, F. Multiwfn: A Multifunctional Wavefunction Analyzer. *J. Comput. Chem.* **2012**, *33*, 580−592.
(47) Website of Multiwfn program. http://Multiwfn.codeplex.com (accessed Jan 28, 2013).
(48) Dean, J. A. *Lange's Handbook of Chemistry (in Chinese)*, 15th ed.; Science Press: Beijing, 2003; pp 4.43−4.54.
(49) Abramowitz, M.; Stegun, I. A. *Handbook of Mathematical Functions with Formulas, Graphs, and Mathematical Tables*; Dover Publications: New York, 1970.
(50) Lebedev, V. I.; Laikov, D. N. A Quadrature Formula for the Sphere of the 131st Algebraic Order of Accuracy. *Dokl. Math.* **1999**, *59*, 477−481.
(51) It is noteworthy that this statement is not always strictly true for other systems. For instance, there may be some potential curves that are anomalously stiff near the equilibrium distance and flatten noticeably farther away, leading to much weaker bond dissociation energies than might be expected.
(52) Gdanitz, R. J. An Accurate Interaction Potential for Neon Dimer (Ne_2). *Chem. Phys. Lett.* **2001**, *348*, 67−74.
(53) Torre, A.; Alcoba, D. R.; Lain, L.; Bochicchio, R. C. Determination of Three-Center Bond Indices from Population Analyses: A Fuzzy Atom Treatment. *J. Phys. Chem. A* **2005**, *109*, 6587−6591.
(54) Chen, Z.; Wannere, C. S.; Corminboeuf, C.; Puchta, R.; Schleyer, P. v. R. Nucleus-Independent Chemical Shifts (NICS) as an Aromaticity Criterion. *Chem. Rev.* **2005**, *105*, 3842−3888.
(55) Becke, A. D.; Edgecombe, K. E. A Simple Measure of Electron Localization in Atomic and Molecular Systems. *J. Chem. Phys.* **1990**, *92*, 5397−5403.
(56) Lu, T.; Chen, F. Meaning and Functional Form of the Electron Localization Function. *Acta Phys. Chim. Sin.* **2011**, *27*, 2786−2792.
(57) Shaik, S.; Danovich, D.; Silvi, B.; Lauvergnat, D. L.; Hiberty, P. C. Charge-Shift Bonding—A Class of Electron-Pair Bonds That Emerges from Valence Bond Theory and Is Supported by the Electron Localization Function Approach. *Chem.—Eur. J.* **2005**, *11*, 6358−6371.
(58) Jensen, F. *Introduction to Computational Chemistry*, 2nd ed.; John Wiley & Sons: West Sussex, U.K., 2007; pp 148−153 and 369.
(59) Lendvay, G. On the Correlation of Bond Order and Bond Length. *J. Mol. Struct.: THEOCHEM* **2000**, *501−502*, 389−393.
(60) Szabo, A.; Ostlund, N. S. *Modern Quantum Chemistry*; Dover Publications: New York, 1989.
(61) Slater, J. C. A Simplification of the Hartree−Fock Method. *Phys. Rev.* **1951**, *81*, 385−390.
(62) Vosko, S. H.; Wilk, L.; Nusair, M. Accurate Spin-Dependent Electron Liquid Correlation Energies for Local Spin Density Calculations: A Critical Analysis. *Can. J. Phys.* **1980**, *58*, 1200−1211.
(63) Perdew, J. P.; Burke, K.; Ernzerhof, M. Generalized Gradient Approximation Made Simple. *Phys. Rev. Lett.* **1996**, *77*, 3865−3868.
(64) Adamo, C.; Barone, V. Toward Reliable Density Functional Methods Without Adjustable Parameters: The PBE0Model. *J. Chem. Phys.* **1999**, *110*, 6158−6170.
(65) Gatti, C. The Source Function Descriptor as a Tool to Extract Chemical Information from Theoretical and Experimental Electron Densities. *Struct. Bonding (Berlin)* **2012**, *147*, 193−285.
(66) Koch, W.; Holthausen, M. C. *A Chemist's Guide to Density Functional Theory*, 2nd ed.; Wiley-VCH Verlag GmbH: Germany, 2001; pp 24−28.